



Selective liquid-phase oxidation of alcohols catalyzed by a silver-based catalyst promoted by the presence of ceria

Matthias J. Beier^a, Thomas W. Hansen^b, Jan-Dierk Grunwaldt^{a,*}

^a Department of Chemical and Biochemical Engineering, Technical University of Denmark, Søtofts Plads, Building 229, DK-2800 Kgs. Lyngby, Denmark

^b Center for Electron Nanoscopy, Technical University of Denmark, DK-2800 Kgs. Lyngby, Denmark

ARTICLE INFO

Article history:

Received 3 April 2009

Revised 23 June 2009

Accepted 25 June 2009

Available online 23 July 2009

Keywords:

Selective alcohol oxidation

Silver catalysis

Molecular oxygen

X-ray absorption spectroscopy

Gold catalysts

Catalyst screening

Ceria

ABSTRACT

A number of silver catalysts supported on SiO₂, Al₂O₃, Celite, CeO₂, kaolin, MgO, and activated carbon were screened for their catalytic activity in the selective liquid-phase oxidation of benzyl alcohol using a special screening approach. For this purpose 5–6 catalyst samples were mixed and tested simultaneously. When a high catalytic conversion (>30% over 2 h) was found the number of catalyst components was reduced in the following tests. Thereby, a collaborative effect between a physical mixture of ceria nanoparticles and silver-impregnated silica (10 wt.% Ag–SiO₂) was found. The catalytic activity was highly dependent on the silver loading, the amount of ceria, and especially the calcination procedure. Transmission electron microscopy (TEM), X-ray diffraction (XRD), and X-ray absorption spectroscopy (XANES, EXAFS) demonstrate that silver is mainly present as metallic particles. This is also supported by *in situ* XAS experiments. Oxygen species incorporated in the silver lattice appear to be important for the catalytic oxidation of the alcohol for which a preliminary mechanism is presented. The application of the catalyst was extended to the oxidation of a wide range of primary and secondary alcohols. Compared to palladium and gold catalysts, the new silver catalyst performed similarly or even superior in the presence of CeO₂. In addition, the presence of ceria increased the catalytic activity of all investigated catalysts.

© 2009 Elsevier Inc. All rights reserved.

1. Introduction

Selective oxidation reactions comprise one of the most important classes of transformations in organic chemistry. The catalytic oxidation of alcohols is especially interesting [1–7] since this reaction can be utilized in the production of aldehydes e. g. useful in the food processing or cosmetics industry. In addition, it has found great interest as one of the key reactions for processing biomass [8–10]. Acknowledging the importance of the oxidation of alcohols under benign conditions, a number of groups have focused on developing economical and ecological reasonable alternatives to the use of toxic chromium(VI) species or specially designed oxidants. Today, both homogeneous catalysts [3,8,11], often utilizing nitroxyl radicals and heterogeneous catalytic systems [12,13], are available for the selective oxidation of a variety of different alcohols to the corresponding carbonyl compounds using preferentially oxygen as oxidant. Heterogeneous catalysts are often based on noble metals such as Pt [14], Ru [15], Pd [16], and Au [17–19] or combinations thereof [20–22] when reactions are performed in liquid or liquid-like phases. While especially the Pt group metals afford high catalytic activities under

mild conditions, gold catalysts have attained wide interest mainly due to their high selectivity toward aldehydes [23]. On the other hand, catalytic activities are often only moderate. Gold catalysts were also used successfully for upgrading such as ethanol as a typical “renewable” into the corresponding acid or ester and proved to be superior when compared to Pt or Pd catalysts [24,25].

However, there are only very few publications reporting silver being catalytically active in the liquid-phase alcohol oxidation [26–30]. This is surprising since silver catalysts are used in many gas-phase oxidations with the most prominent examples being ethylene [31] and methanol oxidation [32]. Early studies report that silver salts supported on, e.g. silica [33] or Celite [34,35] can be used as stoichiometrical and mild oxidizing agents for the selective liquid-phase oxidation of alcohols. Recently, Mitsudome et al. [29] described a silver-ion exchanged hydrocalcite which turned out to be catalytically active in the selective oxidation of primary and secondary alcohols. Interestingly, experiments were performed under anaerobic conditions affording very good selectivities. This demonstrates that silver has a high potential for catalytic oxidation reactions also in the liquid phase.

Thus, we were prompted to assess the potential of silver as a catalyst material for the selective oxidation of alcohols using benzyl alcohol as a model compound. Starting with a screening

* Corresponding author. Fax: +45 4588 2258.
E-mail address: jdg@kt.dtu.dk (J.-D. Grunwaldt).

approach of various silver-impregnated supports we used XRD, XAS, TEM and catalytic studies on various substrates in order to gain a more fundamental understanding of the catalyst structure and a first insight into the reaction mechanism.

2. Experimental

2.1. Catalyst preparation

For screening different silver catalysts, a number of materials were synthesized by impregnation of TiO₂ (Aeroxide P25, Degussa, 50 m²/g), Al₂O₃ (MCO-239U, Haldor Topsøe A/S), SiO₂ (Aerosil 200, Degussa, 200 m²/g), MgO (Sigma-Aldrich, 30 mesh), activated carbon (CAP super, SX plus, CA 1, Darco S-51, all NORIT Nederland B. V.), CeO₂ (Aldrich, <25 nm), and Celite (Celite 500 fine, Fluka) with an aqueous AgNO₃ (Sigma-Aldrich, 99.5%) solution containing the appropriate amount to obtain the targeted weight loading. The mixtures were protected from light and left at room temperature. Typically after 24 h impregnation time, the catalysts were dried at 90 °C for 24 h followed by calcination for 2 h at a temperature between 300 and 700 °C.

For Ag–SiO₂ the preparation conditions were varied leading to the following synthesis protocol: 5.00 g silica (Aerosil 200, Degussa, 200 m²/g) was impregnated with 25 mL of an aqueous solution containing 785 mg AgNO₃ (Sigma-Aldrich, 99.5%). After 72 h impregnation time protected from light at room temperature allowing evaporation of water the catalyst samples were dried in air at 90 °C for 24 h. The catalyst was calcined at 500 °C for 30 min in a muffle oven controlled by a Eurotherm 904 controller. After grinding, a beige powder was obtained. Possible variations to this protocol are described in the corresponding results section.

2.2. Catalyst testing

The catalytic tests were typically carried out by pouring a mixture of 40 mL xylene (mixture of isomers, Aldrich), 2.1 g (2.0 mL, 19 mmol) benzyl alcohol (SAFC, 99%), and 0.10 g biphenyl (Sigma-Aldrich, 99.5%) as internal standard in a three-necked flask equipped with a reflux condenser, a gas inlet, and a magnetic stir bar. The conditions are similar to Ref. [29]. The reaction mixture was heated up to reflux and equilibrated for 15 min. After adding 100 mg Ag–SiO₂ and 50 mg CeO₂ (Aldrich, <25 nm), the solution was continuously saturated with flowing oxygen (Linde, 99.95%). Samples were taken in regular intervals for GC analysis. GC analysis was performed on an Agilent 6890 N gas chromatograph equipped with a 7683 B series autosampler, a flame ionization detector, and a HP Innowax column (30 m × 0.25 mm × 0.25 μm) using biphenyl as an internal standard. Screening experiments were carried out under the same conditions with a grinded mixture of the catalysts. Test reactions with other alcohols were carried out using 1-octanol (Fluka, 99.5%), 2-octanol (Sigma-Aldrich, 97%), 2-methoxybenzyl alcohol (Fluka, 97%), 3-methoxybenzyl alcohol (Aldrich, 98%), 4-methoxybenzyl alcohol (Aldrich, 98%), 1-phenylethanol (Aldrich, 98%), 1-naphthalenemethanol (Aldrich, 98%), cinnamyl alcohol (Fluka, 97%), and cyclohexanol (Fluka, 99%). In addition, competitive experiments were carried out in a mixture of 20 mL xylene, 2.0 mmol of benzyl alcohol, 2.0 mmol of a *p*-substituted benzyl alcohol (4-methoxybenzyl alcohol, 98%; 4-chlorobenzyl alcohol, 99%; 4-thrifylfluoromethylbenzyl alcohol, 98%; all Aldrich) and 0.10 g biphenyl (Sigma-Aldrich, 99.5%) under an oxygen atmosphere using 100 mg of 10% Ag–SiO₂ and 50 mg CeO₂. Evaluation was done according to Ref. [24] within the first 60 min of the experiments to minimize deactivating influences of the products.

2.3. Inductively coupled plasma mass spectrometry (ICP-MS)

A hot solution obtained after 3 h reaction time was filtered through Celite. 5.00 mL of this solution was used for further analysis. After evaporating the organic solvent *in vacuo* over night the residual was dissolved in concentrated HNO₃ and diluted with double distilled water to 10.0 mL. The measurements were performed with an ICP-MS instrument (Perkin–Elmer Elan 5000) equipped with a cross-flow nebulizer. The plasma Ar flow was set to 13 L/min at 800 W RF power and the nebulizer Ar flow was set to 0.80 L/min. The sample solution was injected with 1.4 mL/min. Quantification of Ce and Ag was done using multielement ICP-MS standard solutions (Fluka).

2.4. Characterization

The specific surface area was determined by nitrogen adsorption on an ASAP 2010 (Micromeritics) at liquid nitrogen temperature applying the BET theory. The sample was dried under vacuum at 200 °C for 48 h prior to the measurement.

X-ray diffraction (XRD) was measured with an X'Pert PRO diffractometer (PANalytical) with a Cu-K_α X-ray source operated at 45 kV and 40 mA equipped with a Ni filter and a slit. Diffractograms were recorded between 2θ (Cu-K_α) = 20° and 90° with a step width of 0.00164°. The crystallite size was measured from the FWHM of the Ag(111) reflection using the Debye–Scherrer equation after correction for the instrument broadening.

X-ray absorption spectroscopy (XAS) was measured at the SuperXAS beamline at the Swiss Light Source (SLS, Villigen) and at the X1 beamline at the Hamburger Synchrotronstrahlungslabor (HASYLAB) at the Deutsche Elektronen-Synchrotron (DESY, Hamburg). XAS spectra were recorded in step-scanning mode around the Ag K-edge ($E = 25.514$ keV) with a Si(311) double crystal monochromator in transmission mode by measuring the beam intensity before and after the sample and after the Ag reference foil by ionization chambers. *In situ* studies were performed with the powdered catalyst precursor placed in a glass capillary and heated in an oven as described elsewhere [36]. The glass capillary was open to the environment. The oven was heated from room temperature to 500 °C with 50 °C/min. XANES spectra were processed by energy calibration, background subtraction, and normalization using the WinXAS 3.1 software [37]. EXAFS spectra were extracted from the XAS spectra after analogous treatment and Fourier-transformation between $k = 3$ Å⁻¹ and 13 Å⁻¹. EXAFS fitting was performed in R-space up to 5.5 Å based on the silver lattice structure. The first, second, and third silver shells was fitted assuming a constant damping factor of 0.8. Scattering amplitudes and phase shifts were calculated with the FEFF 7.0 code [38]. Particle sizes were calculated from the fitted first shell coordination number as described in [39] assuming spherical particles. The residual was between 7 and 9.

Transmission electron microscopy data were acquired using an FEI Titan 80–300 image corrected microscope operated at 300 kV and an FEI Tecnai T20 G2 operated at 200 kV. Both microscopes are equipped with Oxford Instruments INCA EDX spectrometers for elemental analysis. Ceria and silver particles were distinguished by measuring lattice spacings and angles between lattice fringes. The particle size distribution was automatically calculated using the ImageJ 1.40 g software package after enhancing the contrast manually. In order to compare the particle sizes derived from the other characterization methods, the contribution of the particles to the XRD and EXAFS by their volume must be taken into account. Thus, the average particle size was calculated from the particle size distribution by weighting the individual particle volume according to Eq. (1).

$$d_{\text{average}} = \frac{\sum_1^n N_j V_j d_j}{\sum_1^n N_i V_i} \quad (1)$$

where d_{average} is the average volume-weighted particle size; N_{ij} is the number of particles with the same diameter; V_{ij} is the volume of particle assuming spherical particles with diameter d ; and d_j is the particle diameter.

3. Results

3.1. Synthesis of silver catalysts and catalyst screening

In order to identify catalysts for alcohol oxidation, a series of silver-containing catalysts were synthesized by impregnation of SiO₂, Al₂O₃, TiO₂, CeO₂, kaolin, MgO, Celite, and activated carbon with 1–10 wt.% silver loading. The catalysts were calcined in air at temperatures between 300 °C and 700 °C and were tested for catalytic activity in the oxidation of benzyl alcohol to benzaldehyde. The reaction was performed under reflux in an oxygen atmosphere using xylene as a solvent. Since during the screening phase of the catalysts only a simple classification as catalytically active/inactive was necessary, 5–6 different catalysts were tested simultaneously in one batch. At this early stage only the conversion of benzyl alcohol was considered since the selectivity is influenced by various materials in the mixture. Selected mixtures to demonstrate the principle are given in Table 1. Most catalyst mixtures resulted only in conversions lower than 10%. However, especially one mixture of catalysts exhibited significantly higher catalytic activity (entry 4; 41% conversion). By reducing the number of catalysts tested in each experiment Ag–SiO₂ and Ag–CeO₂ were identified to be required for obtaining catalytic activity (entry 7). Testing the two catalysts separately gave only small conversions below 5%. In addition, silver impregnation was not necessary on CeO₂ and thus nanostructured CeO₂ (average particle size 25 nm) and 10 wt.% Ag–SiO₂, calcined for 2 h at 500 °C, were ascertained as the key components. Interestingly, catalyst mixtures containing CeO₂ and Ag–SiO₂ calcined at 300 °C, 400 °C, 600 °C, or 700 °C performed distinctively worse. Silver in Ag–SiO₂ calcined at 500 °C was found to be mainly in metallic state as evidenced by XANES/EXAFS (Fig. 1) and XRD (not shown). The near edge structure in the XANES region is similar to silver foil. The Fourier-transformed EXAFS spectrum showed mainly the Ag–Ag backscattering typical for metallic silver. XRD reflections exhibited the typical features of metallic Ag with only a small contribution corresponding to Ag₂O. The specific surface area measured by BET was 180 m²/g.

3.2. Investigation of the collaborative behavior of the Ag–SiO₂/CeO₂ system

Since Ag–SiO₂ and CeO₂ tested alone did not exhibit catalytic activity (conversion <10%) we continued studying the origin of

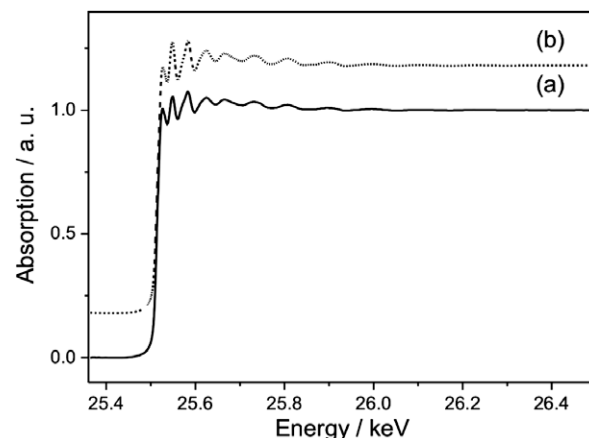


Fig. 1. EXAFS spectrum recorded at the Ag K-edge of a freshly prepared 10 wt.% Ag–SiO₂ catalyst calcined for 2 h at 500 °C (a) compared to silver foil (b).

the collaborative behavior and the preparation procedures for Ag–SiO₂ and CeO₂ in more detail. At first, the influence of the silver loading of Ag–SiO₂ catalysts was studied. A series containing 1–20 wt.% were synthesized by calcination at 500 °C for 2 h and investigated in a mixture with CeO₂. As can be seen in Fig. 2, a silver loading of 10 wt.% gave the highest conversion, while a higher loading resulted in a more selective catalyst. Catalysts with a loading of 1 wt.% did not achieve a significantly higher conversion than a mixture of SiO₂ and CeO₂. The selectivity increased with higher silver loading. As the selectivity is only slightly worse compared to the 20 wt.% sample, further studies were conducted using silica with 10 wt.% silver. The influence of the Ag–SiO₂/CeO₂ ratio on the catalytic activity was investigated keeping the amount of silver constant (Fig. 3). At low CeO₂ contents both catalyst activity and selectivity increased with increasing content of CeO₂. The optimum ratio of was found to be 2:1 (Ag–SiO₂/CeO₂). A ratio of 1:1 (Ag–SiO₂/CeO₂) led reproducibly to a decreased catalytic activity. Both the highest conversion and the highest selectivity were obtained with a mixture of 1:3 (Ag–SiO₂/CeO₂) which, however, seems not preferable as it would refer to 400 mg of catalyst material compared to 150 mg for a 2:1 (Ag–SiO₂/CeO₂) ratio. A reason for the increased catalytic activity with a higher CeO₂ loading might be that water and benzaldehyde are partly adsorbed thereby preventing catalyst deactivation caused by the reaction products (*vide infra*). Intensive mixing of Ag–SiO₂ and CeO₂ by, e.g. grinding was not necessary prior to reaction, so both compounds were added separately to the reaction mixture. Nevertheless, a proximity of Ag–SiO₂ and CeO₂ is necessary. This is indicated by our observation that when CeO₂ and Ag–SiO₂ were packed in separated filter paper containers, the catalytic activity was not higher than Ag–SiO₂ packed in a filter container alone. Additionally, the reaction did not proceed after filtering the hot reaction mixture and adding

Table 1
Selected catalyst mixtures screened for catalytic oxidation of benzyl alcohol. Reaction Conditions: 40 ml xylene, 2.00 mL benzyl alcohol, 0.10 mL ^tbutyl benzene, 50 mg of each catalyst (Ag–SiO₂: 100 mg), O₂ atmosphere, reaction time 3 h.

Entry	T_{calc} (°C)	Catalyst supports and Ag loading (in wt.%)						Conversion of benzyl alcohol (%)	
		SiO ₂	TiO ₂	Al ₂ O ₃	Celite	kaolin	CeO ₂		MgO
1	400	3	3		3		3	3	6
2	500	3	3		3	5	3	3	16
3	600	3	3		3		3	3	2
4	500	10	10	10	10		10		41
5	Uncalc.	10	10	10	10		10		6
6	500		10		10		10		4
7	500	10					10		37

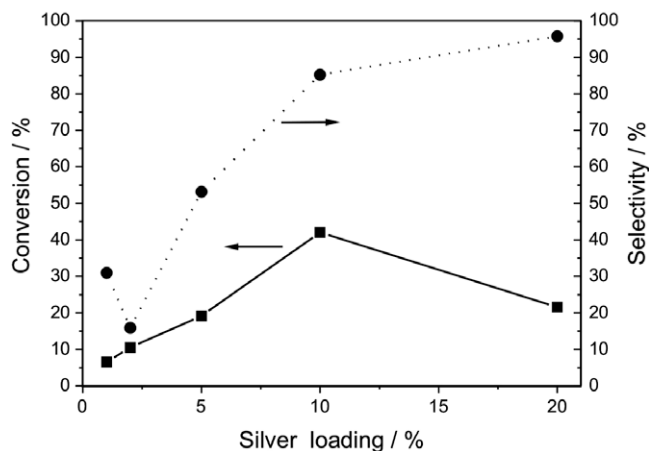


Fig. 2. Conversion (■) and selectivity (●) obtained from Ag–SiO₂ (calcined in air at 500 °C for 2 h) with different silver loadings. Reaction conditions: 40.0 mL xylene, 19.3 mmol benzyl alcohol, 0.20 g biphenyl, 100 mg Ag–SiO₂, 50 mg CeO₂, reflux, O₂ atmosphere, 3 h reaction time. The lines are for the guide of the eye.

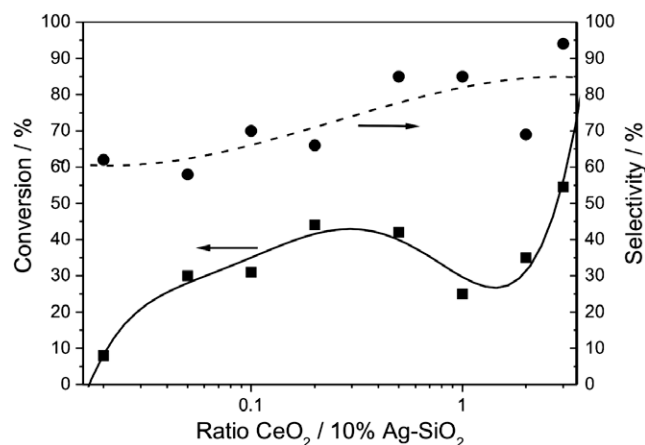


Fig. 3. Conversion (■) and selectivity (●) obtained from Ag–SiO₂ with different CeO₂ to 10% Ag–SiO₂ ratios. Reaction conditions: 40.0 mL xylene, 19.3 mmol benzyl alcohol, 0.20 g biphenyl, 100 mg of 10% Ag–SiO₂ (calcined in air at 500 °C for 2 h) with the indicated CeO₂ content, reflux, O₂ atmosphere, 3 h reaction time. Note that the abscissa is logarithmic. The lines are for the guide of the eye.

either Ag–SiO₂ or CeO₂. Leaching of silver and cerium was low, i.e. concentrations determined with ICP-MS were 0.10 mg/L (± 0.01 mg/L) for silver and 11 μ g/L (± 2 μ g/L) for cerium. Addition of Ce(III) 2-ethylhexanoate to Ag–SiO₂ as a soluble cerium source with a nine times higher cerium concentration of 0.1 mg/L did not result in an enhanced catalytic activity. In accordance, TEM images of *ex situ* samples reacted for 15 min and 300 min, respectively, showed a high dispersion of the CeO₂ nanoparticles on the silica support (Fig. 4c and d). Thus, dissolved Ce or Ag species are not the main reason for the enhanced catalytic activity.

3.3. Influence of the catalyst synthesis and calcination procedure

The catalyst exhibited higher selectivity by increasing the impregnation time prior to drying from 24 h to 72 h. XRD analysis showed a decrease in the mean particle size from 26 nm to 11 nm with longer impregnation time (measured after calcinations at 500 °C). Further screening experiments (*vide supra*) proposed a calcination temperature of 500 °C resulting in a far superior catalyst compared to 400 °C and 600 °C. In order to trace the changes during calcination, we studied the calcination process *in situ* in a glass

capillary (Fig. 5). The catalyst precursor was heated up rapidly at about 50 °C/min from room temperature to 500 °C with the capillary being open to the environment. The first spectrum corresponds to silver in the state of AgNO₃ which is transformed to an intermediate silver species between 300 and 450 °C correlating with the observation of only low conversion (<10%) by the Ag–SiO₂ obtained from calcination at 400 °C. While pure AgNO₃ decomposes to metallic silver above 440 °C, metallic silver was only observed after ca. 20 min at 500 °C. The intermediate species has a similar edge position as the freshly impregnated catalyst precursor, thus silver was mainly in the oxidized state. Note, that the reduction was only observed when the capillary was open to air and not with a flow of 21 vol.% O₂ / He. In a flow of pure He the reduction occurred rapidly at 500 °C.

The XAS studies indicate that calcination time plays an important role. Fig. 6 shows the performance of catalysts calcined between 15 min and 8 h. The catalyst activity increased with calcination time reaching a maximum after 1 h exhibiting, however, the poorest selectivity. Longer calcination times enhanced the selectivity but had an overall negative effect on the observed conversion. A calcination time of 30 min gave the most effective catalyst. The particle size obtained from XRD did not show any trend and was fluctuating between 11 and 16 nm.

3.4. Effects of reaction conditions and reaction time

In order to study the influence of the reaction atmosphere, experiments were performed in flowing oxygen, air, and inert atmosphere (Table 2). The reaction rate is highest in pure oxygen. Decreasing the amount of oxygen led to a lower reaction rate. Anaerobic conditions prevented the formation of any product. During the course of the reaction, the catalyst deactivated gradually. Since benzaldehyde added to the starting mixture decreased the reactant conversion significantly, competitive adsorption on the reaction sites between reactant and product may hinder the product formation. Furthermore, water has an undesired effect on the catalyst performance since both a catalyst treated with water prior to the reaction considerably lost catalytic activity (conversion <2%) and water added during the reaction stopped the product formation. Using a drying agent suitable for high temperatures as in refluxing xylene, i.e. anhydrous MgSO₄ and molecular sieves 3 Å, respectively, a significantly higher degree of conversion at the cost of selectivity was found (Fig. 7). The observed lower selectivity which does not originate from the drying agent alone suggests that water also plays a moderating role by, e.g. blocking highly active sites. Both deactivation by water [40,41] and an increase in selectivity by blocking highly active sites [14,42,43] are not uncommon in alcohol oxidation. After use, the catalyst was significantly less active (conversion 16%, Table 3). Hence, the catalyst deactivation was not reversible. Reactivation of the used catalyst was observed only after addition of fresh Ag–SiO₂ while addition of CeO₂ had no influence, so the deactivation is related to Ag–SiO₂. Calcination of used catalyst at 500 °C for 30 min partly reactivated the catalyst leading to a conversion of 45% after 2 h (Table 3). In order to gain insight into the changes during the reaction we prepared a number of spent catalyst samples reacted between 15 min and 5 h and investigated those using *ex situ* XAS (Fig. 8). Comparing the XANES region of these samples we found only a slight change of the catalyst during reaction. The Fourier-transformed EXAFS spectra showed a pronounced increase in the magnitude of the peak corresponding to 1st shell Ag–Ag backscattering between fresh and used catalysts. The difference in magnitude is largest within the first 15 min and increases slightly with higher reaction times but does not reach that of silver foil. The coordination number of the first shell obtained from EXAFS data fitting increased from fresh catalyst to used catalyst to silver foil (Table 4 and Fig. 9). Estimation

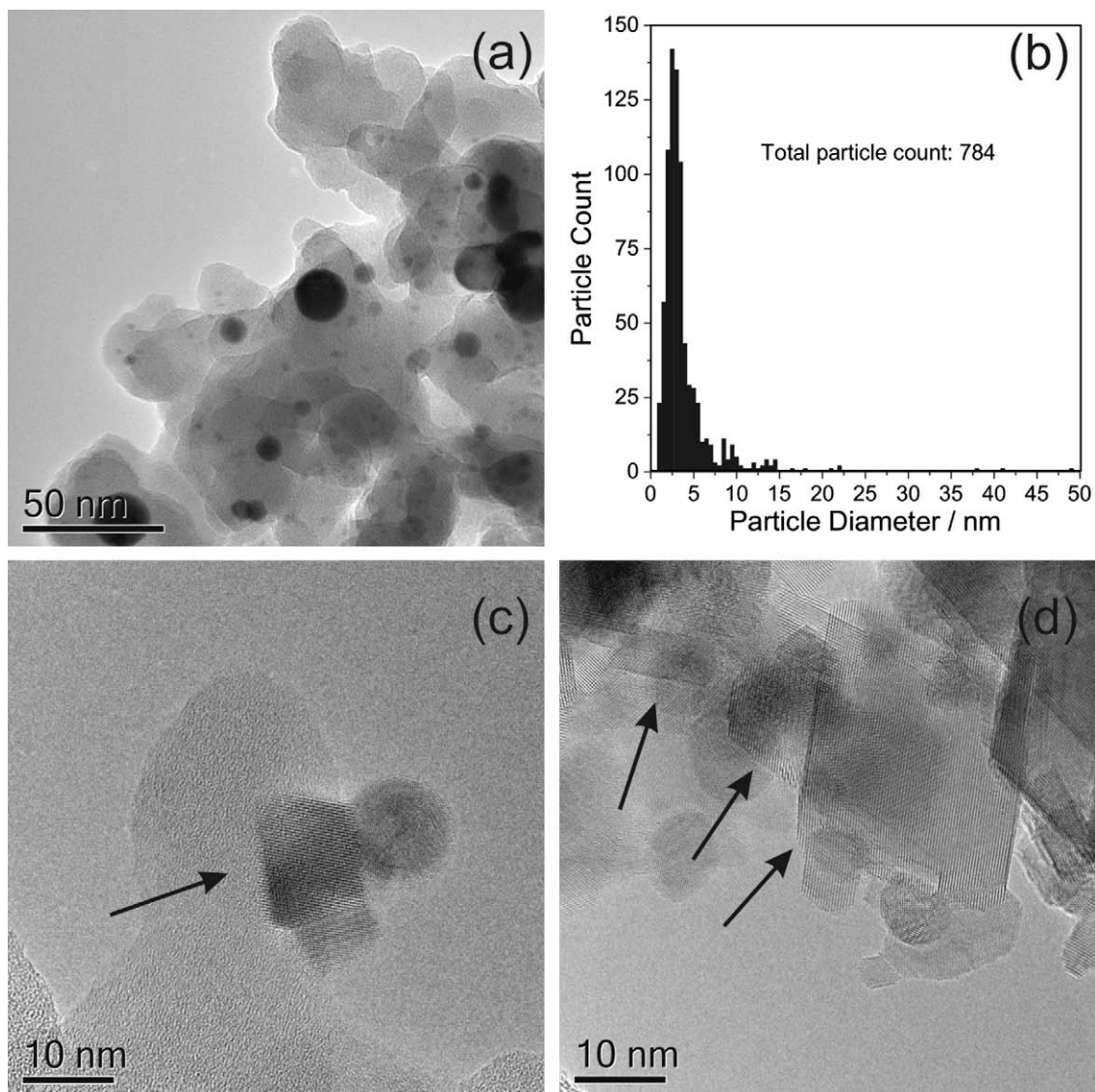


Fig. 4. TEM images of freshly calcined 10% Ag-SiO₂ prior to mixing with CeO₂ (a) and corresponding particle size distribution of freshly calcined 10% Ag-SiO₂ (b). Catalyst mixture of 10% Ag-SiO₂ and CeO₂ after 15 min (c) and 300 min (d) reaction time. Arrows indicate CeO₂ nanoparticles. Dark circles are silver particles on the silica support (verified with EDX).

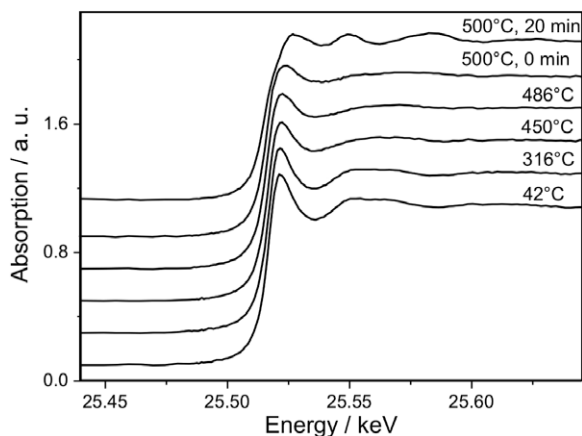


Fig. 5. *In situ* XANES spectra recorded at the Ag K-edge during calcination of 10% Ag-SiO₂ in air in an open quartz capillary without gas flow.

of the particle size from EXAFS results in a cluster size of ca. 1.5 nm for the fresh catalyst and 3 nm for the catalyst after 15 min reaction time which are both significantly lower than the particle size obtained from XRD (29 nm). TEM evaluation proves that most particles are in the range of 2–3 nm, which might be X-ray amorphous (Fig. 4b). However, TEM also shows significantly larger particles with some particles even in the range of 50 nm. Since both XRD and EXAFS give a volume-weighted particle size, large particles have a significantly higher influence on the average particle size. A volume-weighted particle size of 33 nm was calculated from the TEM data which is in good agreement with XRD results. Note, however, that the influence of large particles on the average volume-based particle size is high. Table 5 summarizes particle sizes obtained from XRD, EXAFS, and TEM. Obviously, the particle size from EXAFS appears to be significantly underestimated. It can be excluded that very small clusters or isolated silver atoms not observable with TEM contribute significantly to the EXAFS function since these would give different backscattering contributions. An explanation for this discrepancy in the EXAFS results is either imperfections in the lattice or the involvement of silver oxygen

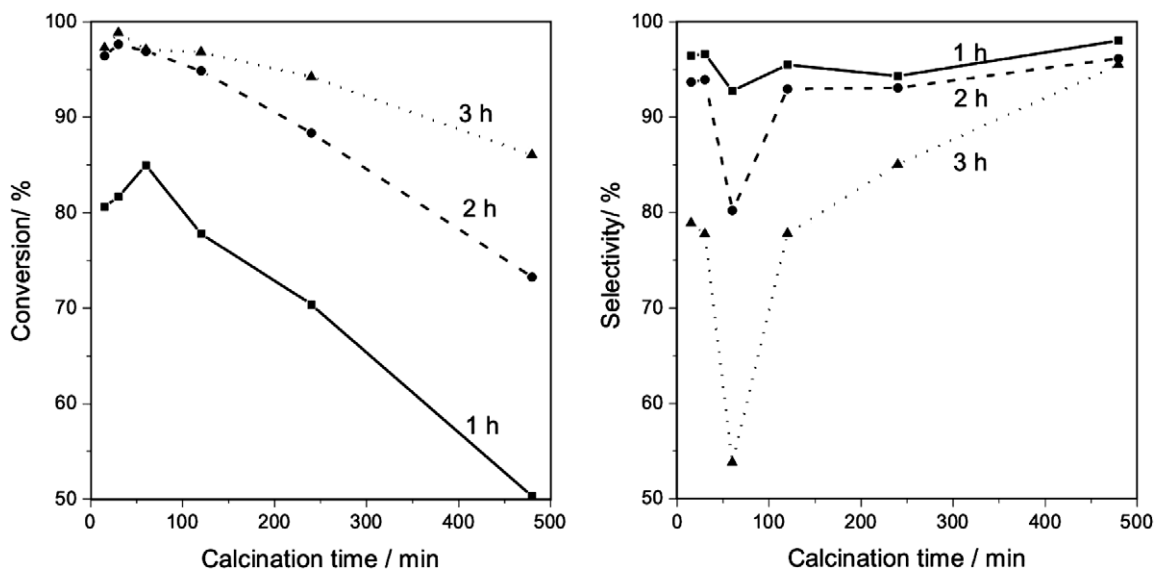


Fig. 6. Conversion and selectivity depending on the calcination time after 1 h, 2 h, and 3 h. Reaction conditions: 20.0 mL xylene, 2.0 mmol benzyl alcohol, 0.10 g biphenyl, 50 mg of 10% Ag–SiO₂, 25 mg CeO₂, reflux, O₂ atmosphere, reaction time as indicated.

Table 2

Conversion and selectivity over 10% Ag–SiO₂ promoted with CeO₂ under different reaction atmospheres. Reaction conditions: 20.0 mL xylene, 0.10 g biphenyl, 2.00 mmol alcohol, 50 mg of 10% Ag–SiO₂, 25 mg CeO₂, 2 h reflux in atmosphere as indicated.

	Flowing O ₂	Air	Flowing N ₂ ^a
Conv. (%)	98	15	<1
Sel. (%)	95	94	Traces

^a Reaction mixture purged for 30 min prior to reaction.

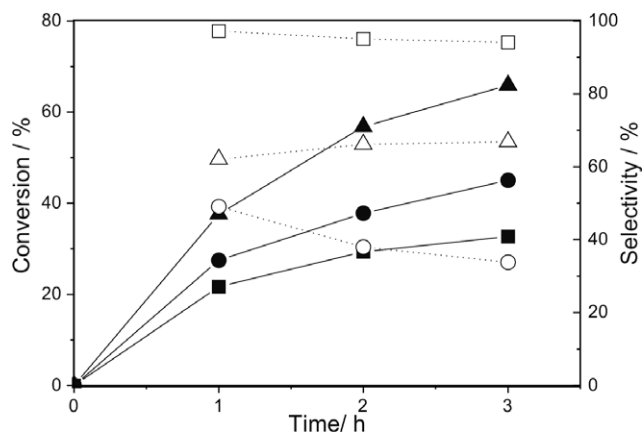


Fig. 7. Conversion and selectivity depending on the addition of a drying agent: conversion and selectivity without addition of drying agent (■, □), with molecular sieves 3 Å (▲, △) and MgSO₄ (●, ○). Reaction conditions: 40.0 mL xylene, 19.3 mmol benzyl alcohol, 0.20 g biphenyl, 100 mg of 10% Ag–SiO₂, 50 mg CeO₂, reflux in O₂ atmosphere.

Table 3

Conversion and selectivity of a fresh, used, and re-calcined CeO₂ promoted 10% Ag–SiO₂ catalyst (500 °C, 30 min in air). Reaction conditions: 20.0 mL xylene, 0.10 g biphenyl, 2.00 mmol alcohol, 50 mg of 10% Ag–SiO₂, 25 mg CeO₂, 2 h reflux in oxygen atmosphere.

	Fresh catalyst	Used catalyst	Re-calcined catalyst
Conv. (%)	98	16	45
Sel. (%)	95	>99	93

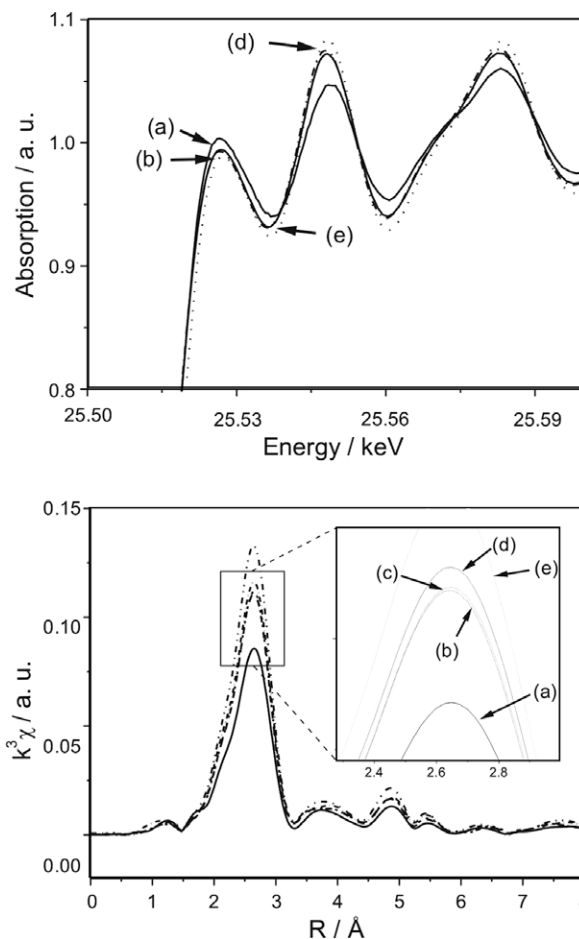


Fig. 8. XANES (top) and Fourier-transformed EXAFS (bottom) spectra of *ex situ* 10% Ag–SiO₂/CeO₂ (2:1) catalyst samples before reaction (a), after 15 min (b), 90 min (c), and 5 h (d), reaction time, and (e) silver foil.

species. Oxygen dissolved in silver (β -oxygen) is known to cause disorder in the silver lattice [44]. If an intercalated species does not lie on the axis between absorber atom and reflecting atom

Table 4
Structural parameters obtained from EXAFS data fitting.

Sample	Ag–Ag shell	<i>N</i>	<i>R</i> (Å)	σ^2 (Å ⁻²)
Ag foil	1	12	2.86 ^a	0.009
	2	6	4.03	0.011
	3	24	5.03	0.015
10% Ag–SiO ₂	1	7.9	2.86 ^a	0.009
	2	6.0 ^b	4.01	0.014
	3	4.2	5.04	0.007
10% Ag–SiO ₂ /CeO ₂ after 15 min	1	10	2.86 ^a	0.009
	2	6.0 ^b	4.01	0.013
	3	5.0	5.03	0.006

^a Note that the Ag–Ag distance found is by 0.03 Å too small which is in analogy to examples found in the literature [68].

^b Coordination number was constrained to 6.0.

Table 5

Overview over the average diameter of silver particles of 10% Ag–SiO₂ (calculated at 500 °C for 2 h) obtained from XRD, EXAFS, and TEM.

Characterization method	XRD	EXAFS	TEM
Particle size/nm	29	1.5	2.5 ^a

^a Most abundant particle size.

^b Average particle size calculated from Eq. (1).

[45,46] it will have a decreasing effect on the inelastic electron mean free path length thereby attenuating the EXAFS amplitude significantly even at low dopant concentrations [47,48] which might be the case in this study. Note that the oxygen content is presumably too undefined to be observable directly via Ag–O backscattering.

3.5. Extension to further alcohols and comparison to other noble metal catalysts

In order to broaden the application of the novel silver-based catalyst system, the alcohol oxidation reaction was extended to a number of primary and secondary alcohols (Table 6) and compared to other well-described catalyst systems. 10% Ag–SiO₂ calcined for 30 min at 500 °C mixed with CeO₂ in a 2:1 ratio was used as an optimized catalyst for this purpose. Secondary alcohols were oxidized to the corresponding ketones with high selectivity and high conversion for the oxidation of 1-phenylethanol within just 45 min, while the oxidation of 2-octanol afforded moderate yields after 3 h reaction time. The oxidation of cyclohexanol produced a considerable amount of a not identified side product. Primary alcohols were in general also oxidized with high selectivity to the aldehyde while the conversions depended on the reactants to a high extent. The oxidation of 1-octanol commenced with a high initial rate. With reaction times longer than 1 h, the selectivity to octanal decreased significantly favoring the formation of octanoic acid.

The silver-based catalyst was compared with three impregnated gold catalysts and one Pd catalyst based on the same catalyst weight for the oxidation of benzyl alcohol (Table 7) both with and without the addition of CeO₂ in the absence of a base. Without CeO₂, Ag–SiO₂ is highly selective but gives only very low conversions. Remarkably, the observed conversions for all catalysts increased with addition of CeO₂. Thus, Pd–Al₂O₃ afforded almost full conversion already after 30 min, with, however, only low selectivity, while combination with CeO₂ was crucial for the activity of silver catalyst achieving both high selectivity and conversion after 2 h (cf. Table 7). The gold catalysts underwent deactivation during the course of the reaction, i.e. longer reaction times resulted in only slightly higher conversions at the cost of selectivity. Note, however, that here reaction conditions optimized for the silver catalyst were used.

Alcohol oxidation on Pt group metals [12] and on Au [24] is believed to occur via hydride abstraction thus involving an intermediate cationic species. Comparing the conversion of benzyl alcohol with *para*-substituted benzyl alcohols in a competitive experiment [24], we found that electron withdrawing substituents decreased the reaction rate while electron donating substituents had a beneficial effect (Table 8). This supports that also in this case the rate limiting step involves the formation of a cationic species.

4. Discussion

In this study we focused on silver-based catalysts to investigate whether they can be used as alternatives for other noble metal catalysts such as the recently widely reported gold-based catalysts. By screening several catalysts simultaneously in one batch, we found

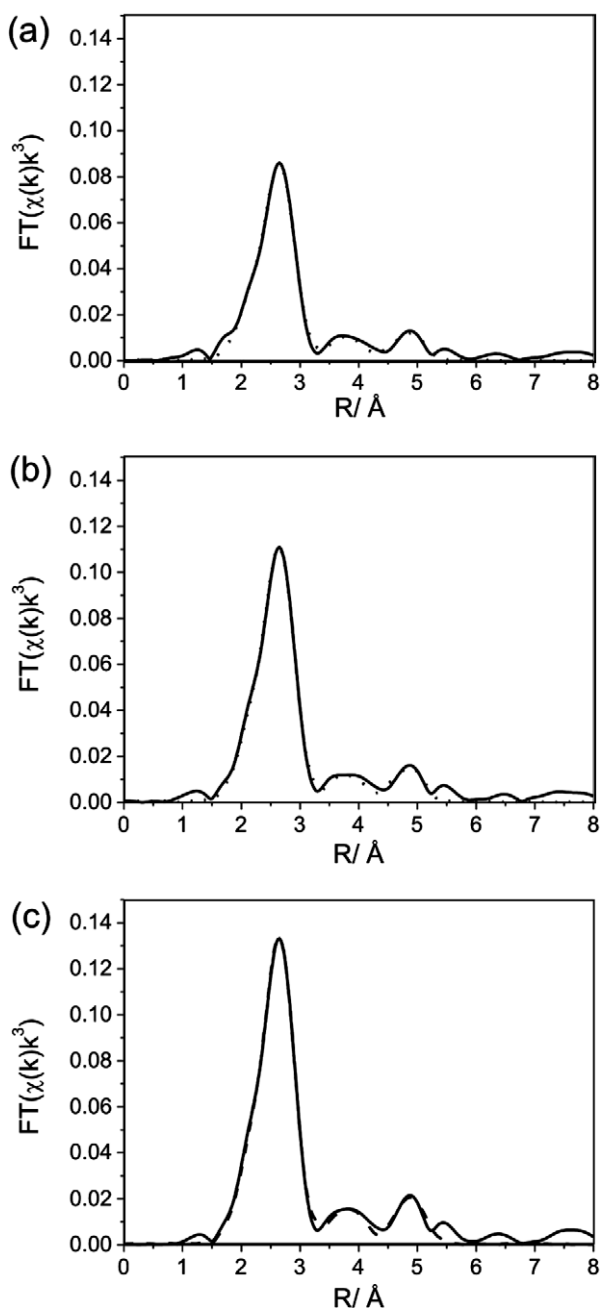
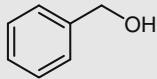
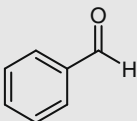
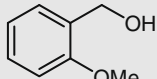
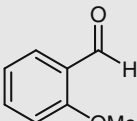
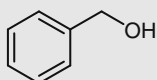
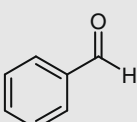
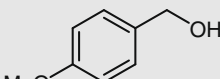
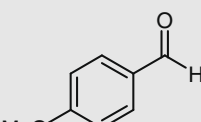
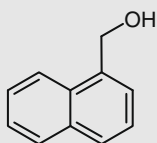
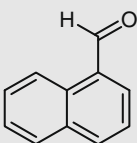
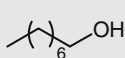
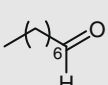
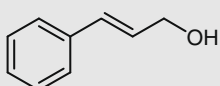
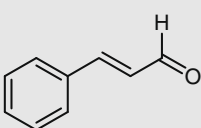
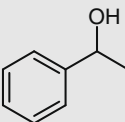
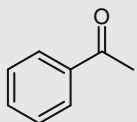
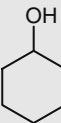
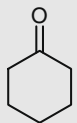


Fig. 9. Experimental (solid line) and fitted (dashed line) radial distribution function of fresh 10% Ag–SiO₂ catalyst (a), 10% Ag–SiO₂ catalyst after 15 min reaction time (b) and silver foil (c). EXAFS data fits were made up to 5.5 Å for the first three Ag shells.

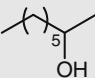
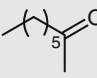
Table 6

Oxidation of various primary and secondary alcohols catalyzed by 10% Ag–SiO₂ and CeO₂. Reaction conditions: 20.0 mL xylene, 0.10 g biphenyl, 2.00 mmol alcohol, 50 mg Ag–SiO₂, 25 mg CeO₂, reflux in O₂ atmosphere.

Entry	Substrate	Product	Time (h)	Conv. (%)	Sel. (%)
1			2	98	95
2			3	90	>99
3			3	92	>99
4			3	83	>99
5			3	39	99
6			0.75 ^a	29	90
7			3	83	97
8			0.75	>99	>99
9			2	22	71

(continued on next page)

Table 6 (continued)

Entry	Substrate	Product	Time (h)	Conv. (%)	Sel. (%)
10			2	63	>99

^a Longer reaction times decreased the selectivity considerably.

a novel Ag–SiO₂ catalyst that acts as efficient catalyst but only in the presence of ceria. Often such screening of catalysts is performed by parallel and even robot-controlled high-throughput units requiring sophisticated equipment [49,50]. For the identification of new catalyst materials, however, qualitative results are often sufficient in preliminary studies which allows for a highly simplified test strategy. This simple test strategy can be regarded as an alternative to single catalyst testing requiring no special instrumentation. A similar approach is used in the split-pool method [51,52]. However, inhibition or synergetic interactions between the catalyst materials cannot be excluded. In fact, we found a synergism between Ag–CeO₂ and Ag–SiO₂ calcined at 500 °C using this screening strategy. This combination of catalysts led to a much higher conversion (>35%, Table 1) than all the other supported silver catalysts which exhibited only poor catalytic activity. A more detailed investigation showed that the use of CeO₂ instead of Ag–CeO₂ was sufficient.

The most active catalyst was identified to be a 1:2 mixture of CeO₂ nanoparticles and 10 wt.% Ag–SiO₂ calcined for 30 min at 500 °C. Ag–SiO₂ without CeO₂ reacted considerably slower (Table 7) and requires harsher conditions to facilitate benzyl alcohol oxidation at which only poor selectivities are obtained [30]. Since the reaction products deactivated the catalyst, the substrate/catalyst ratio had to be adapted to achieve full conversion. Comparison of the optimized silver catalyst reported herein to standard gold and palladium catalysts showed that all catalysts became more active by addition with CeO₂ under the chosen reaction conditions (Table 7). Silver and palladium benefitted more from the addition than the corresponding gold catalysts. Palladium became highly reactive with a low selectivity, the silver catalyst maintained its high selectivity at almost full conversion. In contrast the latter gave hardly any conversion in the absence of CeO₂. In light of these studies, silver offers a worthy alternative to well-established noble metals especially when considering that silver is less expensive.

Unlike gold, which is catalytically active on many different supports [23], our screening experiments found a large number of silver catalysts to be virtually inactive under the chosen reaction conditions. This reflects the present status of the literature since there are significantly less reports on silver catalysts than for gold-based catalysts in selective oxidation reactions in liquid phase. It can be expected that silver was in metallic state on all supports after calcination above 600 °C. Since most catalysts gave conversions <5% (Table 1) metallic silver alone cannot be the active phase. There are several points suggesting that silver–oxygen spe-

cies in mostly metallic silver particles play an important role. Silver strongly interacts with oxygen. The formation of different silver–oxygen species highly depends on the pretreatment conditions [44,53–56] which play a key role in the gas-phase oxidation of methanol [57,58]. Silver oxygen species are classified corresponding to their thermal desorption behavior into α -oxygen (surface adsorbed), β -oxygen (bulk oxygen), and γ -oxygen (subsurface oxygen). On metallic silver these species form at temperatures above 500 °C upon exposure with oxygen [55]. Significantly higher temperatures as well as treatment in hydrogen decrease the amount of adsorbed α - and β -oxygen which was already found for Ag–SiO₂ in a CO oxidation study [59,60]. This coincides both with our observation that calcination temperatures higher than 500 °C have a negative effect on the catalytic activity and other catalytic studies reported on silver impregnated pumice in alcohol oxidation [26]. Another indication for the involvement of oxygen species is the virtual disagreement in particle size obtained from XRD, EXAFS, and TEM. XRD and TEM suggest an average volume-based particle size in the range of 30 nm making the particle size of less than 2 nm obtained from EXAFS data obviously highly underestimated. Intercalated oxygen species fitting well in the octahedral gaps of the fcc metal [56] could serve as an explanation.

An important finding is that the oxidation pathway does not involve homogeneous catalysis by dissolved cerium or silver species. The concentrations of both components as found with ICP-MS were low and a hot filtered solution did not continue reacting, even when either CeO₂ or Ag–SiO₂ was added. In addition, only low conversions below 10% were observed, when both CeO₂ and Ag–SiO₂ were separated from each other (and not well mixed). Finally, higher amounts of CeO₂ have a positive effect on the catalytic performance. Hence, like for other noble metals [61–64], alcohol oxidation occurs on the heterogeneous catalyst probably on the silver particles. As for gold [65] the higher reactivity of electron-rich ben-

Table 8

Comparison of reaction rate constants based on the conversion of *para*-substituted benzyl alcohols with respect to benzyl alcohol. Reaction conditions: xylene 20.0 mL, 2.00 mmol benzyl alcohol, 2.00 mmol *p*-substituted benzyl alcohol, 0.10 g biphenyl, 100 mg of 10% Ag–SiO₂, 50 mg CeO₂, reflux in oxygen atmosphere.

<i>para</i> -substituent	–CF ₃	–Cl	–OMe
k_X/k_H^a	0.18	0.24	1.6

^a Ratio of 1st-order rate constants based on the conversion of *p*-substituted benzyl alcohol (k_X) and benzyl alcohol (k_H).

Table 7

Comparison of the optimized Ag catalyst with Pd and Au catalysts. Conditions: 20 mL xylene, 0.10 g biphenyl, 2.00 mmol benzyl alcohol, 50 mg catalyst, 2 h reflux in O₂ atmosphere.

	10% Ag–SiO ₂	1% Au–ZnO	1% Au–Al ₂ O ₃	1% Au–TiO ₂	0.5% Pd–Al ₂ O ₃
Conv. (%)	6	45	72	24	81
Sel. (%)	>99	90	90	91	67
<i>Catalyst with CeO₂ (25 mg)</i>					
Conv. (%)	98	75	77	39	94 ^a
Sel. (%)	95	93	93	99	58 ^a

^a Reaction time: 30 min.

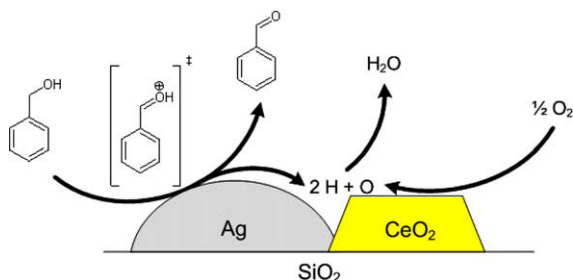


Fig. 10. Schematic and simplified reaction mechanism. Benzyl alcohol oxidation occurs via adsorption of benzyl alcohol on silver, dehydrogenation at the silver surface followed by desorption of benzaldehyde. Hydrogen is removed from the silver surface by means of atomic oxygen provided by the CeO_2 -silver interface.

zyl alcohols suggests a positively charged reaction intermediate formed by hydride abstraction. Unlike silver-modified hydrotalcite [29], our catalyst requires oxygen to be catalytically active which emphasizes the role of CeO_2 . A beneficial effect of ceria as a support material has been found before [20,66–71]. The role of CeO_2 may be to act as an oxygen pool as it is capable of reversibly storing oxygen [72]. Fig. 10 gives a schematic overview over the reactions occurring on the catalyst: after adsorption of benzyl alcohol on the silver surface the alcohol is dehydrogenated forming a cationic intermediate reacting further to benzaldehyde. CeO_2 activates molecular oxygen which reacts with hydrogen from benzyl alcohol thereby regenerating the silver surface. Thus, analogies between the liquid-phase alcohol oxidation on silver and the extensively investigated oxidation on palladium and gold catalysts appear reasonable. In future, further studies, e.g. by ATR-IR as known for palladium-catalysts [73–75] should be performed to corroborate the suggested mechanism, to understand the collaborative effect between silver and ceria in detail, and to shed more light on the deactivation mechanism.

5. Conclusions

A variety of silver catalysts could be effectively screened for the selective oxidation of alcohols by a simple one-batch approach for which different catalyst materials were mixed and tested together. In this way, we found a physical mixture of ceria nanoparticles and silver-impregnated silica to be catalytically active due to cooperative effects occurring during this screening approach. 10 wt.% Ag- SiO_2 mixed with ceria nanoparticles in a ratio of 2:1 gave the best catalytic performance. An important parameter was the calcination temperature being optimal at 500 °C. This is probably due to the temperature dependency of the formation of metallic silver oxygen species which are likely to be involved in the catalytic process as indicated by EXAFS, XRD, and TEM. At too high temperatures oxygen dissolved in metallic silver desorbs whereas at too low calcination temperatures mainly oxidized silver species were obtained. The negative effect of electron withdrawing groups in the benzyl alcohol oxidation suggests a mechanism where metallic silver as other noble metals acts as main component for the dehydrogenation via a cationic intermediate. Dissolved cerium species as the origin of the promoting effect can be excluded. Its role can rather be ascribed to the activation of molecular oxygen. Comparing CeO_2 modified Ag- SiO_2 with Au and Pd catalysts, silver serves as a promising alternative being less expensive and both applicable to a wide variety of alcohols. Interestingly, a positive effect of CeO_2 was also found for Au and Pd catalysts. Therefore, further studies should be devoted to unraveling the promoting effect of ceria in the future.

Acknowledgments

This study is supported by DTU, the Graduate School MP2T and Haldor Topsøe A/S. We thank Alexander Gese for synthetic assistance and Helge Rasmussen for assistance during the XRD experiments. Haldor Topsøe A/S, the group of Professor Baiker (ETH Zurich), Evonik Degussa GmbH, and Norit Nederland BV are acknowledged for donation of support materials. HASYLAB at DESY, Hamburg and SLS at the Paul-Scherrer-Institute, Villigen, are acknowledged for beamtime and financial support (Contract RII13-CT-2004-506008) the World Gold Council for donation of the gold reference catalysts. Finally, we thank Samira Telschow (DTU-KT) for measuring BET surface areas, the Chastine and Maersk Mc-Kinney Møller foundation for funding the Center for Electron Nanoscopy and Jens Enevold Thaulov Andersen (DTU Kemi) for performing the ICP-MS measurements.

References

- [1] T. Mallat, A. Baiker, *Catal. Today* 19 (1994) 247.
- [2] M. Besson, P. Gallezot, *Catal. Today* 57 (2000) 127.
- [3] J. Muzart, *Tetrahedron* 59 (2003) 5789.
- [4] K. Kaneda, K. Ebitani, T. Mizugaki, K. Mori, *Bull. Chem. Soc. Jpn.* 79 (2006) 981.
- [5] A.S.K. Hashmi, G.J. Hutchings, *Angew. Chem. Int. Ed.* 45 (2006) 7896.
- [6] A. Corma, H. Garcia, *Chem. Soc. Rev.* 37 (2008) 2096.
- [7] G.J. Hutchings, *Chem. Commun.* (2008) 1148.
- [8] P.L. Bragd, H. van Bekkum, A.C. Besemer, *Top. Catal.* 27 (2004) 49.
- [9] M. Comotti, C. Della Pina, E. Falletta, M. Rossi, *J. Catal.* 244 (2006) 122.
- [10] J.N. Chheda, G.W. Huber, J.A. Dumesic, *Angew. Chem. Int. Ed.* 46 (2007) 7164.
- [11] R.A. Sheldon, I.W.C.E. Arends, *Adv. Synth. Catal.* 346 (2004) 1051.
- [12] T. Mallat, A. Baiker, *Chem. Rev.* 104 (2004) 3037.
- [13] T. Matsumoto, M. Ueno, N. Wang, S. Kobayashi, *Chem. Asian J.* 3 (2008) 196.
- [14] T. Mallat, Z. Bodnar, A. Baiker, O. Greis, H. Strubig, A. Reller, *J. Catal.* 142 (1993) 237.
- [15] Z. Opre, J.-D. Grunwaldt, M. Maciejewski, D. Ferri, T. Mallat, A. Baiker, *J. Catal.* 230 (2005) 406.
- [16] M. Caravati, J.-D. Grunwaldt, A. Baiker, *Catal. Today* 91-92 (2004) 1.
- [17] D.I. Enache, J.K. Edwards, P. Landon, B. Solsona-Espriu, A.F. Carley, A.A. Herzing, M. Watanabe, C.J. Kiely, D.W. Knight, G.J. Hutchings, *Science* 311 (2006) 362.
- [18] H. Miyamura, R. Matsubara, Y. Miyazaki, S. Kobayashi, *Angew. Chem. Int. Ed.* 46 (2007) 4151.
- [19] P. Haider, B. Kimmeler, F. Krumeich, W. Kleist, J.-D. Grunwaldt, A. Baiker, *Catal. Lett.* 125 (2008) 169.
- [20] A. Abad, P. Concepcion, A. Corma, H. Garcia, *Angew. Chem. Int. Ed.* 44 (2005) 4066.
- [21] S. Marx, A. Baiker, *J. Phys. Chem. C* 113 (2009) 6191.
- [22] N. Dimitratos, J.A. Lopez-Sanchez, D. Morgan, A.F. Carley, R. Tiruvalam, C.J. Kiely, D. Bethell, G.J. Hutchings, *Phys. Chem. Chem. Phys.* 11 (2009) 5142.
- [23] C. Della Pina, E. Falletta, L. Prati, M. Rossi, *Chem. Soc. Rev.* 37 (2008) 2077.
- [24] C.H. Christensen, B. Jorgensen, J. Rass-Hansen, K. Egeblad, R. Madsen, S.K. Klitgaard, S.M. Hansen, M.R. Hansen, H.C. Andersen, A. Riisager, *Angew. Chem. Int. Ed.* 45 (2006) 4648.
- [25] B. Jorgensen, S.E. Christiansen, M.L.D. Thomsen, C.H. Christensen, *J. Catal.* 251 (2007) 332.
- [26] L.F. Liotta, A.M. Venezia, G. Deganello, A. Longo, A. Martorana, Z. Schay, L. Gucci, *Catal. Today* 66 (2001) 271.
- [27] P. Nagaraju, M. Balaraju, K.M. Reddy, P.S. Sai Prasad, N. Lingaiah, *Catal. Commun.* 9 (2008) 1389.
- [28] S. Rakovsky, S. Nikolova, L. Dimitrov, L. Minchev, J. Ilkova, *Oxidation Commun.* 18 (1995) 407.
- [29] T. Mitsudome, Y. Mikami, H. Funai, T. Mizugaki, K. Jitsukawa, K. Kaneda, *Angew. Chem. Int. Ed.* 47 (2008) 138.
- [30] F. Adam, A.E. Ahmed, S.L. Min, J. Porous Mater. 15 (2008) 433.
- [31] X.E. Verykios, F.P. Stein, R.W. Coughlin, *Cat. Rev. Sci. Eng.* 22 (1980) 197.
- [32] H. Sperber, *Chem. Ing. Tech.* 41 (1969) 962.
- [33] T. Nishiguchi, F. Asano, *J. Org. Chem.* 54 (1989) 1531.
- [34] M. Fetizon, M. Golfier, *Acad. Sci. Ser. C* 267 (1968) 900.
- [35] F.J. Kakis, M. Fetizon, N. Douchkin, M. Golfier, P. Mourgues, T. Prange, *J. Org. Chem.* 39 (1974) 523.
- [36] J.-D. Grunwaldt, M. Caravati, S. Hannemann, A. Baiker, *Phys. Chem. Chem. Phys.* 6 (2004) 3037.
- [37] T. Ressler, *J. Synchrotron Radiat.* 5 (1998) 118.
- [38] S.I. Zabinsky, J.J. Rehr, A. Ankudinov, R.C. Albers, M.J. Eller, *Phys. Rev. B* 52 (1995) 2995.
- [39] A. Jentys, *Phys. Chem. Chem. Phys.* 1 (1999) 4059.
- [40] M. Burgener, T. Tyszewski, D. Ferri, T. Mallat, A. Baiker, *Appl. Catal. A* 299 (2006) 66.
- [41] B. Kimmeler, J.-D. Grunwaldt, A. Baiker, *Top. Catal.* 44 (2007) 285.
- [42] H. Kimura, K. Tsuto, T. Wakisaka, Y. Kazumi, Y. Inaya, *Appl. Catal. A* 96 (1993) 217.

- [43] M. Wenkin, P. Ruiz, B. Delmon, M. Devillers, *J. Mol. Catal. A* 180 (2002) 141.
- [44] B. Pettinger, X. Bao, I. Wilcock, M. Muhler, R. Schlögl, G. Ertl, *Angew. Chem. Int. Ed.* 33 (1994) 85.
- [45] B. Lengeler, *Solid State Commun.* 55 (1985) 679.
- [46] B. Lengeler, *Phys. Rev. Lett.* 53 (1984) 74.
- [47] S. Emura, K. Koto, A. Yoshiasa, H. Ito, S. Gonda, S. Mukai, *J. Mater. Sci. Lett.* 8 (1989) 1236.
- [48] E.A. Stern, B.A. Bunker, S.M. Heald, *Phys. Rev. B* 21 (1980) 5521.
- [49] T. Zech, G. Bohner, O. Laus, J. Klein, M. Fischer, *Rev. Sci. Instrum.* 76 (2005) 062215.
- [50] D. Farrusseng, *Surf. Sci. Rep.* 63 (2008) 487.
- [51] M.A. Aramendia, V. Borau, C. Jiménez, J.M. Marinas, F.J. Romero, F.J. Urbano, *J. Catal.* 209 (2002) 413.
- [52] Y.P. Sun, B.C. Chan, R. Ramnarayanan, W.M. Leventry, T.E. Mallouk, S.R. Bare, R.R. Willis, *J. Comb. Chem.* 4 (2002) 569.
- [53] C. Rehren, G. Isaac, R. Schlögl, G. Ertl, *Catal. Lett.* 11 (1991) 253.
- [54] C. Rehren, M. Muhler, X. Bao, R. Schlögl, G. Ertl, *Z. Phys. Chem.* 174 (1991) 11.
- [55] X. Bao, M. Muhler, B. Pettinger, R. Schlögl, G. Ertl, *Catal. Lett.* 22 (1993) 215.
- [56] A.J. Nagy, G. Mestl, D. Herein, G. Weinberg, E. Kitzelmann, F. Schlogl, *J. Catal.* 182 (1999) 417.
- [57] H. Schubert, U. Tegtmeier, D. Herein, X. Bao, M. Muhler, R. Schlögl, *Catal. Lett.* 33 (1995) 305.
- [58] X. Bao, M. Muhler, R. Schlögl, G. Ertl, *Catal. Lett.* 32 (1995) 185.
- [59] Z.P. Qu, W.X. Huang, M.J. Cheng, X.H. Bao, *J. Phys. Chem. B* 109 (2005) 15842.
- [60] Z.P. Qu, M.J. Cheng, W.X. Huang, X.H. Bao, *J. Catal.* 229 (2005) 446.
- [61] M. Caravati, J.-D. Grunwaldt, A. Baiker, *Phys. Chem. Chem. Phys.* 7 (2005) 278.
- [62] C. Keresszegi, T. Burgi, T. Mallat, A. Baiker, *J. Catal.* 211 (2002) 244.
- [63] A. Abad, A. Corma, H. Garcia, *Chem. Eur. J.* 14 (2008) 212.
- [64] J.-D. Grunwaldt, M. Caravati, A. Baiker, *J. Phys. Chem. B* 110 (2006) 25586.
- [65] P. Fristrup, L.B. Johansen, C.H. Christensen, *Catal. Lett.* 120 (2008) 184.
- [66] A.N. Petryakov, *Catal. Lett.* 28 (1996) 239.
- [67] A.N. Petryakov, N.E. Bogdanchikova, A. Knop-Gericke, *Catal. Today* 91–92 (2004) 49.
- [68] P.R. Sarode, K.R. Priolkar, P. Bera, M.S. Hegde, S. Emura, R. Kumashiro, *Mater. Res. Bull.* 37 (2002) 1679.
- [69] S. Imamura, H. Yamada, K. Utani, *Appl. Catal. A* 192 (2000) 221.
- [70] K. Ebitani, H.-B. Ji, T. Mizugaki, K. Kaneda, *J. Mol. Catal. A* 212 (2004) 161.
- [71] L. Kundakovic, M. Flytzani-Stephanopoulos, *J. Catal.* 179 (1998) 203.
- [72] A. Trovarelli, G.J. Hutchings (Eds.), *Catalysis by Ceria and Related Materials*, Imperial College Press, London, 2002.
- [73] T. Burgi, M. Bieri, *J. Phys. Chem. B* 108 (2004) 13364.
- [74] C. Keresszegi, D. Ferri, T. Mallat, A. Baiker, *J. Phys. Chem. B* 109 (2005) 958.
- [75] C. Mondelli, D. Ferri, J.-D. Grunwaldt, F. Krumeich, S. Mangold, R. Psaro, A. Baiker, *J. Catal.* 252 (2007) 77.